Microstructure evaluations of carbon nanotube/diamond/silicon carbide nanostructured composites by size–strain line-broadening analysis methods

2007 J. Phys.: Condens. Matter 19 356205

(http://iopscience.iop.org/0953-8984/19/35/356205)

IOP PUBLISHING JOURNAL OF PHYSICS: CONDENSED MATTER

J. Phys.: Condens. Matter **19** (2007) 356205 (8pp) doi:10.1088/0953-8984/19/35/356205

Microstructure evaluations of carbon nanotube/diamond/silicon carbide nanostructured composites by size–strain line-broadening analysis methods

Yuejian Wang[1] **and T W Zerda**

Department of Physics and Astronomy, Texas Christian University, Fort Worth, TX 76129, USA

E-mail: yuejianw@lanl.gov and t.zerda@tcu.edu

Received 16 April 2007, in final form 16 July 2007
Published 2 August 2007
Online at stacks.iop.org/JPhysCM/19/356205

Abstract

Efforts have been made to manufacture novel composite materials with improved properties by incorporating multi-wall carbon nanotubes (MWNTs) into metal or brittle ceramic. Here we prepared dense MWNT/diamond/silicon carbide (SiC) composites under high-pressure and high-temperature (HPHT) conditions by anchoring MWNTs into a diamond/SiC matrix. The measured mechanical properties indicate that the composites have both superior hardness and enhanced fracture toughness. Moreover, we have undertaken an x-ray diffraction line-broadening analysis to elucidate how the microstructures including domain sizes and micro-strains depend on the externally applied temperature and how the microstructures correlate to the macroproperties of the as-fabricated composites.

(Some figures in this article are in colour only in the electronic version)

1. Introduction

For many decades, diamond composites, e.g. diamond–SiC composites, have been commercially used in making mining tools, drill bits, and other such items, because of their extreme hardness and excellent wear resistance [1–3]. However, although many manufacturing approaches have been developed to synthesize diamond composites, the low fracture toughness and high brittleness unfortunately greatly restrict their practical application in harsh environments. Long-term efforts have been made to enhance the fracture toughness by reducing the grain sizes of matrix materials from microsize to nanoscale [4–8]. Zhao *et al* [9] showed experimental evidence that reduction of the average size of SiC crystallites from tens of microns down to about 20 nm increased the fracture toughness of diamond/SiC composites.

[1] Present address: LANSCE-LC, MS-H805, Los Alamos National Laboratory, USA.

Table 1. Mechanical properties of specimens. Uncertainty of the results is indicated by values in parentheses.

Samples	Sintering temperature (K)	$\langle x \rangle_{vol}$ (nm) Diamond	SiC	Density (g cm^{-3})	Vickers hardness H_V (GPa)	Fracture toughness K_{IC} (MPa m$^{1/2}$)
C1	1570	269(24)	—	2.283	11(2)	—
C2	1770	332(24)	118(11)	2.488	24(1)	4.0(2)
C3	1920	314(48)	167(18)	3.123	43(5)	8.8(2)
C4	2070	299(32)	225(19)	3.226	42(3)	8.6(1)

After the discovery of carbon nanotubes, their extraordinary mechanical properties, such as Young's modulus as high as 1 TPa [10, 11] and high strain to failure, substantially attracted attention from all of the related scientific and industrial fields. Carbon nanotubes open a promising window to improve and tailor the mechanical properties of materials for specific uses. Carbon nanotubes have been embedded into ceramic, e.g. SiC [12, 13] and alumina [14], to improve the damage tolerance of microcrack initiation and propagation, thus enhancing the fracture toughness of the whole material. The experimental results verified that carbon nanotubes, either single-wall or multi-wall phases, are an ideal reinforcement for ceramic composites [12–14]. In a previous investigation [12], SiC/MWNT composites were successfully synthesized from precursors of MWNTs and nano-silicon under HPHT conditions. The measured values showed a distinct improvement in fracture toughness; however, the relatively lower hardness does not fully satisfy the requirements for potential use in structural applications.

In this current study, MWNT/diamond/SiC composites were synthesized from precursors of diamond, silicon (Si), and MWNTs under high pressure and varied temperatures. The diamond grains embedded into the MWNT skeleton were responsible for the hardness enhancement in comparison with previously synthesized SiC/MWNT composites. On the other hand, MWNTs combined with SiC, which serves as a bonding agent to form strong adhesion between diamond and MWNTs, can reinforce the composites with respect to the fracture toughness. Therefore the novel nanostructured composites are expected to possess both high hardness and enhanced fracture toughness.

2. Experimental details

2.1. Sample preparation

Four samples, C1 to C4 as listed in table 1, were fabricated under 5 GPa and various temperatures from a mixture of diamond powders with grain size of 5–10 μm (General Electric Co.), Si powders with a grain size distribution of 30–70 nm, and MWNTs with outer layer diameter from 10 to 30 nm. Both silicon and MWNTs were purchased from Nanostructured and Amorphous Materials Inc., NM. The initial mixtures of diamond, silicon, and MWNTs with a weight ratio of 78:17:5 were prepared using ultrasonic wet dispersion for 2 h and then by applying mechanical rolling mixing for 72 h.

Sintering experiments were run in a toroidal anvil cell using a 250 ton hydraulic press. Diamond/Si/MWNT mixtures were packed inside a cylindrical graphite heater placed inside the high-pressure cell. The pressure was measured directly by a pressure gauge with a precision of about 0.1 GPa and the temperature was measured by a thermocouple placed inside the specimen with accuracy better than 25 K. The experiments were performed according to the following protocol. The pressure was raised to 5 GPa at room temperature. Then the temperature was

increased to the desired value of 2070 K at a rate of 200 K s^{-1}. The samples were kept at that final temperature for 30 s, after which the temperature was decreased to room temperature and the pressure was released.

2.2. Sample characterization

The x-ray diffraction (XRD) technique was used to identify the phase composition and investigate the microstructure of the specimens. X-ray diffraction patterns were recorded with a Philips diffractometer with Cu Kα_1 radiation ($\lambda = 1.540\,56$ Å), operated at 35 kV and 30 mA. The measurement range of 2θ was from 20° to 110°, and the exposure time was 3 s at each step of 0.02°. To determine and remove the effects of instrumental broadening, a large Si crystal with minimal line broadening supplied by the diffractometer manufacturer was measured to create an instrument calibration file which was used to normalize the observed diffraction line profiles. This procedure was developed by Howard and Snyder [15].

The Vickers hardness and fracture toughness measurements were performed on a Buehler Micromet 2003 tester. We made five measurements on each sample and then took the average values as the final results. Under a loading force of 9.8 N, no cracks emerged at the corners of the indentation marks. The fracture toughness was tested with a larger loading force of 147 N.

2.3. Procedure for evaluation of the x-ray diffraction profiles

X-ray diffraction line-broadening analysis is becoming progressively more popular for microstructure determination. There are a variety of methods developed to realize this goal, such as the integral–breadth method, Fourier methods, and so on. To date, it is generally believed that a Voigt-function approximation for both size-broadening and strain-broadening profiles is a better model to reliably extract the pertinent information of domain sizes and microstrains from the refined profile width parameters of an x-ray diffraction pattern. Balzar and co-workers [16–20] have made significant contributions toward making this technique friendly and convenient by editing the SLH software which was used in present investigation. By refining the physical broadening of the diffraction profiles of the specimens, individual size and distortion integral breadths of Cauchy (β_{SC} and β_{DC}) and Gauss (β_{SG} and β_{DG}) components were obtained, and based on these values the surface- and volume-weighted domain sizes are directly expressed by the following equations:

$$\langle D\rangle_s = \frac{1}{2\beta_{SC}} \tag{1}$$

$$\langle D\rangle_v = \frac{\exp(k^2)}{\beta_{SG}}\mathrm{erfc}(k) \tag{2}$$

where $k = \beta_{SC}/(\pi^{1/2}\beta_{SG})$ is the characteristic integral–breadth ratio of a Voigt function and erfc(k) is the error function complement. As well, the microstrains in crystals can be calculated from the average distance L perpendicular to the diffracting planes and parameters β_{DC} and β_{DG}:

$$\langle \varepsilon^2(L)\rangle = \frac{1}{s_0^2}\left(\frac{\beta_{DG}^2}{2\pi} + \frac{\beta_{DC}}{\pi^2}\frac{1}{L}\right). \tag{3}$$

3. Results

Figure 1 shows the XRD patterns of initial mixtures and composites C1 and C2. The diamond phase appears in every pattern, and the intensities of the diamond peaks do not change very

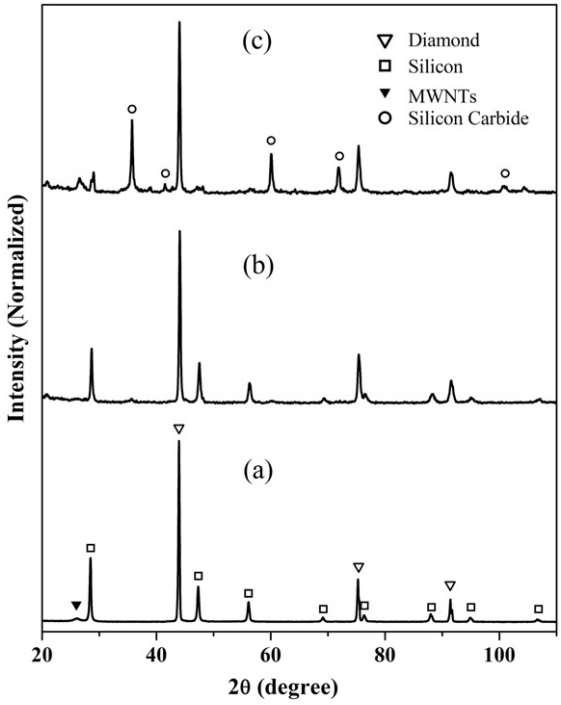

Figure 1. X-ray diffraction patterns: (a) initial mixture; (b) sample sintered at 5 GPa and 1570 K, C1; (c) sample sintered at 5 GPa and 2070 K, C4.

much with temperature. Owing to the small amount of SiC produced in C1, only a tiny hump exists at the reflection position of SiC(111), but the SiC yield increases with temperature elevation. Another phenomenon worth noting is that MWNTs are detected in all specimens, and we do not observe any graphite or amorphous carbon from the x-ray spectra.

The peak widths of diamond and SiC phases in composites demonstrate a reverse trend which can be determined by contrasting figures 3 and 4. Additionally, figure 5 compares the variation of SiC(111) reflections at different temperatures. The diamond precursor has very small peak widths, and then with increasing temperature, the diamond peaks become broadened. In contrast, all of the peaks of the SiC phases are narrower at high temperatures. We also noted unsymmetrical band shapes and smaller shoulders in the SiC diffractograms.

All of the XRD spectra were refined by the double-Voigt multiple-line integral–breadth method. As an example, the fit for the composites formed at 1920 K is shown in figure 2. The tiny differences between measured data and fitted values indicate that the applied simulation methods are accurate and reliable. Based on the profile refinements, the domain sizes and microstrains of diamond and SiC phases have been derived, and the results are depicted in figure 6 and table 1.

The domain sizes of diamond decrease with increasing temperature, but they do not change significantly. However, in the case of SiC phases, the crystallites grow rapidly with elevating temperature. For example, at the highest temperature the diamond domain size decreases by less than 20%, whereas the SiC domain size increases by more than 90%. The microstrain of diamond increases continuously with temperature up to 1920 K and then abruptly drops. As expected, we observe the continuous reduction in magnitude of remaining strain in SiC over the entire scope of the study temperatures. We calculated the domain size and microstrain of the initial diamond. The microstrain of the initial diamond has been plotted in figure 6. Here we provide the domain size of initial diamond, 369 (26) nm, which was not listed in table 1.

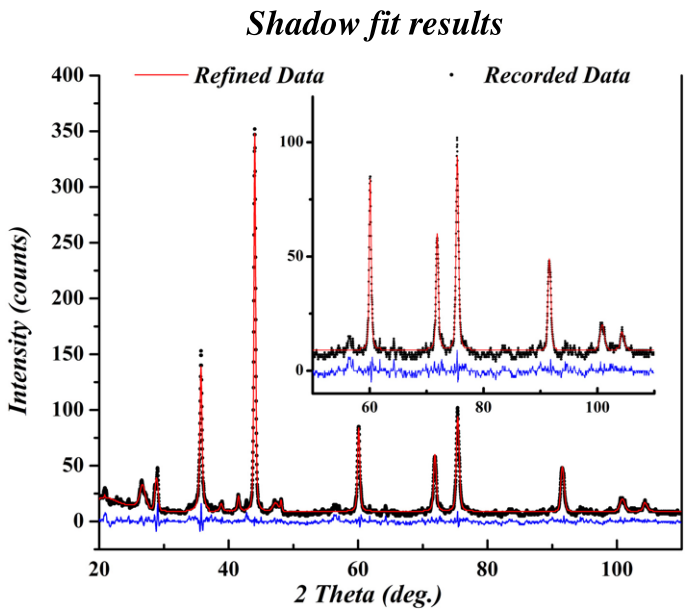

Figure 2. Whole powder pattern fitting and difference plot for sample C4. Line profiles are refined with the Voigt function. The inset shows the enlarged fitted plot of the high-angle region.

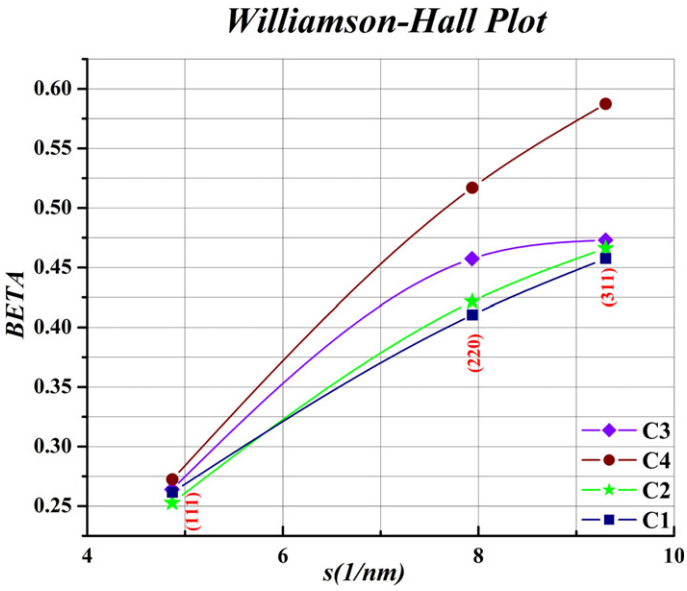

Figure 3. Williamson–Hall plot for diamond phases in samples C1, C2, C3, and C4.

Because the amount of the SiC phase in sample C1 is too small to give an accurate result, we did not consider it in the microstructure analysis.

Data on hardness, fracture toughness, and density are listed in table 1. The table shows that all the measured hardnesses, fracture toughnesses, and densities increase with the temperature. For the samples synthesized at temperatures 1920 and 2070 K, there is very little difference between them.

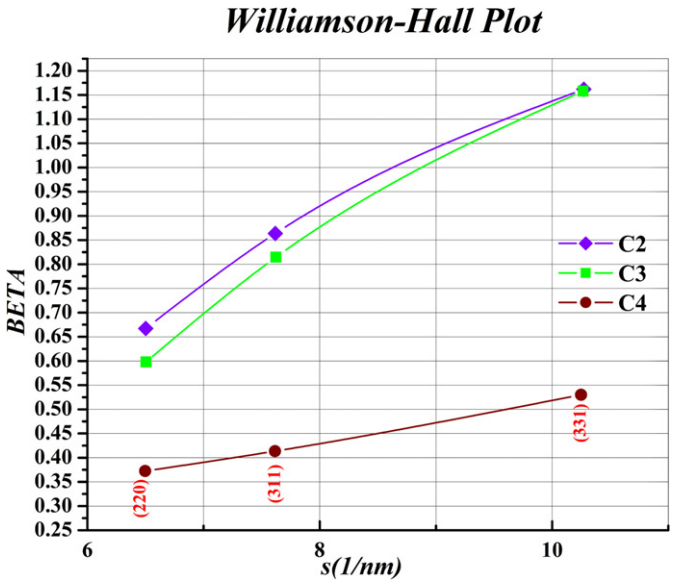

Figure 4. Williamson–Hall plot for SiC phases in samples C2, C3, and C4.

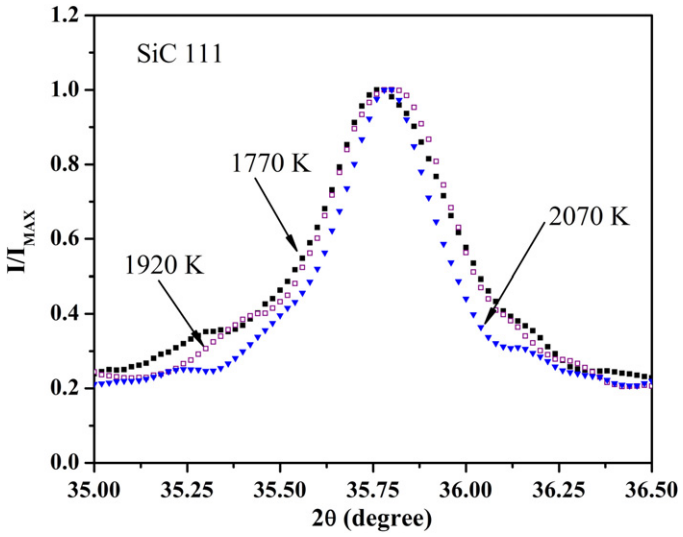

Figure 5. The (111) line profiles of the SiC phases produced at different temperatures.

4. Discussions and summary

Since diamond crystals are broken into smaller size crystallites and additionally some carbon atoms react with silicon, they become smaller under HPHT compared to the original ones. The plausible explanation may exist in the intense plastic deformation of diamond during heating at high pressure [21]. Although some diamond grains sintered together and formed aggregated polycrystallites, this happened only in a smaller number of diamond crystals. For SiC growth, as expected at higher temperatures, atoms of carbon and Si possess more kinetic energy and participate in a reaction which leads to high SiC yield. These phenomena have been confirmed by XRD spectra.

The small shoulder on the lower portion of the (111) peak is due to stacking faults formed during SiC formation under HPHT conditions. In the case of diamond, a large fraction of

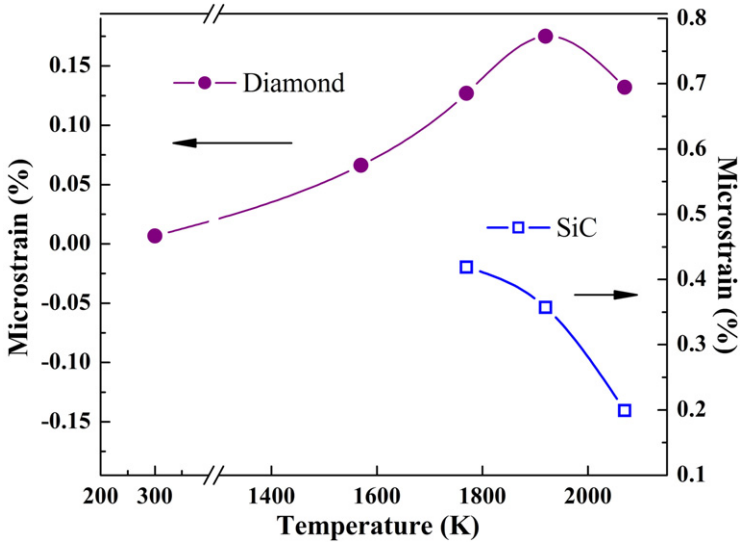

Figure 6. Plot of microstrain in diamond and SiC versus temperature. The computations of microstrains in phases of diamond and SiC were performed on the distance L in the range 12–1600 Å.

the defects is expected to be concentrated at the contact points between two crystals, and the mobility of dislocations becomes intense with increasing temperature [21]. At higher temperatures, some dislocations may migrate into the interior of the crystal, and new defects would grow near the crystal contacting surfaces. Consequently, the population of dislocations increases with temperature. At the highest temperature (2070 K), since the dislocations and vacancies in the surface layer of diamond are almost completely consumed by the carbon–silicon reaction, the dislocations in diamond are annihilated. For SiC phases produced at higher temperature, the decrease in dislocation density and the growth of crystals result in smaller peak widths, but here we cannot define accurately which effect contributes most to this phenomenon.

A higher specimen density indicates that at higher temperatures silicon fills more pores or voids between diamond crystals to form denser composites. Moreover, the high temperature would excite Si and C atoms and expedite the reaction between them. Although the mechanism of reaction between MWNTs and Si under HPHT conditions is not clearly understood, based on the x-ray spectra, it is reasonable to presume that the reactions start from the defects on the surface of MWNTs and continue until they are completely covered by thick SiC layers which block the further diffusion of Si and C atoms. These processes produce a specific structure of MWNTs coated by SiC in which the outer layers of the MWNTs transform into SiC but the inner part of the MWNTs are still left intact. Besides the reaction taking place between MWNTs and Si, Si also reacts with diamond, but it requires more activation energy [22]. The SiC produced from reactions of Si with MWNTs and diamond could act as a good adhesive agent to bond MWNTs and diamond particles together and eventually form a dense and strong composite. Higher temperatures, leading to stronger Si–C bonds and better MWNT/SiC networks, are a persuasive explanation for the super-mechanical properties generated at higher temperature.

The intimate contact among MWNTs, diamond and SiC makes it possible to transfer the load to the carbon nanotubes and prevent the further propagation of cracks. Also, the superior elasticity of carbon nanotubes ingrained in the composites could work as damping to

absorb vibration energy and reduce the intensity of externally applied shock waves. The high Young's modulus of carbon nanotubes alone with the mobility reduction of cracks results in an improvement in fracture toughness of the composites.

Compared to MWNT/SiC composites, the improvement in hardness of the MWNT/diamond/SiC composites was not at the expense of fracture toughness. The measured values of mechanical properties show that, using MWNT/SiC composites as a reference, the hardness of MWNT/diamond/SiC is enhanced as much as 60%, whereas the fracture toughness is still kept at a similar level. The enhancement of hardness is attributed to the involvement of diamond in composite synthesis.

In summary, our study demonstrates that carbon nanotubes are a promising candidate to manufacture nanostructured diamond composites with advanced properties. One thing we may mention here is that both composites of MWNT/diamond/SiC and MWNT/SiC were fabricated at pressures of 5 GPa, lower than that of the usual diamond composite synthesis conditions. More homogeneously dispersing carbon nanotubes within the starting materials may help to make the reaction conditions more attainable, e.g., the use of lower pressure and temperature. This is because the uniform distribution of carbon nanotubes is instrumental in forming an effective network structure in the composites.

Acknowledgments

We thank Brad Shurter for his helpful reviewing and comments. This study was supported by the grant NSF-DMR 0502136.

References

[1] Tomlinson P N, Pipkin N J, Lammer A and Burnand R P 1985 *Diamond Rev.* **6** 299
[2] Tillmann W 2000 *Int. J. Refract. Met. H.* **18** 301
[3] Clark I E and Bex P A 1999 *Ind. Diamond Rev.* **1** 43
[4] Shulzhenko A A, Gargin V G, Bochechka A A, Oleinik G S and Danilenko N V 2000 *J. Superhard Mater.* **22** 1
[5] Veprek S 1999 *J. Vac. Sci. Technol.* A **17** 2401
[6] Andrievski R A 2001 *Int. J. Refract. Met. H.* **19** 447
[7] Ekimov E A, Gavriliuk A G, Palosz B, Gierlotka S, Dluzewski P, Tatianin E, Kluev Yu, Naletov A M and Presz A 2000 *Appl. Phys. Lett.* **77** 954
[8] Gubicza J, Ungár T, Wang Y, Voronin G, Pantea C and Zerda T W 2006 *Diamond. Relat. Mater.* **15** 1452
[9] Zhao Y, Qian J, Daemen L, Pantea C, Zhang J and Zerda T W 2004 *Appl. Phys. Lett.* **84** 1356
[10] Yakobson B I, Brabec C J and Bernholc J 1996 *Phys. Rev. Lett.* **76** 2511
[11] Yu M, Files B S, Arepalli S and Ruoff R S 2000 *Phys. Rev. Lett.* **84** 5552
[12] Wang Y, Voronin G A, Winiarski A and Zerda T W 2006 *J. Phys.: Condens. Matter* **18** 275
[13] Ma R Z, Wu J, Wei B Q, Liang J and Wu D H 1998 *J. Mater. Sci.* **33** 5243
[14] Zhan G, Kuntz J D, Wan J and Mukherjee A K 2003 *Nat. Mater.* **2** 38
[15] Howard S A and Snyder R L 1989 *J. Appl. Crystallogr.* **22** 238
[16] Balzar D 1995 *J. Appl. Crystallogr.* **28** 244
[17] Balzar D and Ledbetter H 1997 *Adv. X-ray Anal.* **39** 457
[18] Balzar D 1992 *J. Appl. Crystallogr.* **25** 559
[19] Balzar D and Ledbetter H 1993 *J. Appl. Crystallogr.* **26** 97
[20] Balzar D 1999 *International Union of Crystallography Monographs on Crystallography No. 10* ed R L Snyder, H J Bunge and J Fiala (Oxford: Oxford University Press) p 94
[21] Pantea C, Gubicza J, Ungár T, Voronin G and Zerda T W 2002 *Phys. Rev.* B **66** 094106
[22] Wang Y and Zerda T W 2006 *J. Phys.: Condens. Matter* **18** 2995